First-Principles Theory of Anharmonicity and the Inverse Isotope Effect in Superconducting Palladium-Hydride Compounds

Ion Errea,[1,2] Matteo Calandra,[1] and Francesco Mauri[1]

[1]*Université Pierre et Marie Curie, CNRS, IMPMC, 4 Place Jussieu, 75252 Paris, France*
[2]*IKERBASQUE, Basque Foundation for Science, 48011 Bilbao, Spain*

Palladium hydrides display the largest isotope effect anomaly known in the literature. Replacement of hydrogen with the heavier isotopes leads to higher superconducting temperatures, a behavior inconsistent with harmonic theory. Solving the self-consistent harmonic approximation by a stochastic approach, we obtain the anharmonic free energy, the thermal expansion, and the superconducting properties fully *ab initio*. We find that the phonon spectra are strongly renormalized by anharmonicity far beyond the perturbative regime. Superconductivity is phonon mediated, but the harmonic approximation largely overestimates the superconducting critical temperatures. We explain the inverse isotope effect, obtaining a -0.38 value for the isotope coefficient in good agreement with experiments, hydrogen anharmonicity being mainly responsible for the isotope anomaly.

The explanation of the ion-mass isotope effect in phonon-mediated superconductors is one of the greatest successes of the Bardeen-Cooper-Schrieffer (BCS) theory [1]. In a BCS superconductor composed of only one type of ions of mass M, the superconducting critical temperature T_c is expected to behave as $T_c \propto M^{-\alpha}$, where $\alpha = 0.5$ is the isotope coefficient. In conventional superconductors with more atomic species, the total isotope coefficient should also be close to 0.5. However, in many superconductors like MgB_2 [2], fullerides [3], or high-T_c cuprates [4,5] the isotope coefficient is substantially reduced and, in the most extreme case of palladium hydrides (PHs), it is even negative [6–8].

An isotope coefficient $\alpha = 0.5$ relies on the following assumptions: (i) the phonon frequencies are harmonic; consequently (ii) the electron-phonon interaction is mass independent, and (iii) the electron-electron interaction is not affected by the isotope substitution. Thus, a reduced isotope effect can either be the fingerprint of a nonconventional mechanism (e.g., spin fluctuations or correlated superconductivity) or the breakdown of one of these assumptions (e.g., anharmonicity). In both cases, the superconducting state is considered anomalous and current state-of-the-art calculations do not quantitatively account for the behavior of T_c as a function of the isotope mass. This is due to the difficulties of dealing either with nonconventional mechanisms or with anharmonicity.

Here we consider the most pathological case present in the literature, the inverse isotope effect in PHs. PdH has $T_c = 8$–9 K [6,7]. Hydrogen substitution with the heavier deuterium leads to a higher T_c, as $T_c(\mathrm{PdD}) \approx 10$–11 K [6,7], leading to $\alpha = -[\ln T_c(\mathrm{PdD}) - \ln T_c(\mathrm{PdH})]/\ln 2 \approx -0.3$. Remarkably, PdT has a higher T_c than PdD, but there is no experimental value at full stoichiometry [8]. A considerable theoretical and experimental effort [9–21] has

been devoted to explaining this phenomenon over the last decades. Karakozov *et al.* [9], in a pioneering work, studied anharmonicity in PHs in the framework of perturbation theory to the bare harmonic phonon frequency and concluded that the negative isotope effect could be due to anharmonicity, as other authors suggested later [19]. Other explanations based on electronic properties [16], zero-point motion [21], and volume effects [20] have been invoked as well. Inelastic neutron scattering experiments [14] show strongly temperature dependent phonon lifetimes, a clear fingerprint of anharmonicity. Furthermore, *ab initio* total energy calculations [18,19] suggest that the potential felt by the hydrogen atoms is very anharmonic. Nevertheless, no state-of-the-art calculations of the electron-phonon interaction and anharmonicity are present so that the interplay of these effects is still unclear.

In this work we study the occurrence of phonon-mediated superconductivity in PHs and show that the inverse isotope effect is quantitatively explained by the inclusion of anharmonicity. Anharmonicity is so large that perturbative approaches [9,22–24] are not feasible in PHs. To solve this issue, we implement the self-consistent harmonic approximation (SCHA) [25] within a first-principles approach. Differently from other methods developed to deal with anharmonic effects [26–28], our method allows us to access directly the anharmonic free energy of the system, with full inclusion of the anharmonic potential terms, and is variational in the free energy with respect to a trial harmonic potential. Moreover, compared to other implementations of the SCHA [29,30], we replace the cumbersome calculation of anharmonic coefficients by the evaluation of atomic forces on supercells with suitably chosen stochastic ionic configurations.

The ionic Hamiltonian is $H = T + V$, where T and V are the kinetic and potential energy operators. In the adiabatic approximation the potential is defined by the

Born-Oppenheimer (BO) energy surface. Then, the free energy of the ionic system can be calculated as $F_H = -\frac{1}{\beta} \ln Z_H$, where the partition function is $Z_H = \text{tr}[e^{-\beta H}]$ and $\beta = 1/(k_B T)$. A quantum variational principle in the free energy can be established for an arbitrary trial Hamiltonian $\mathcal{H} = T + \mathcal{V}$ as [25]

$$F_H \le \mathcal{F}_H[\mathcal{H}] = F_{\mathcal{H}} + \int d\mathbf{R}[V(\mathbf{R}) - \mathcal{V}(\mathbf{R})]\rho_{\mathcal{H}}(\mathbf{R}), \tag{1}$$

where $\rho_{\mathcal{H}}(\mathbf{R}) = \langle \mathbf{R}|e^{-\beta\mathcal{H}}|\mathbf{R}\rangle/Z_{\mathcal{H}}$ is the probability to find a system described by $\mathcal{H}$ in a general $\mathbf{R}$ ionic configuration. The equality holds for $\mathcal{H} = H$. The SCHA takes a harmonic $\mathcal{V}$ and minimizes $\mathcal{F}_H[\mathcal{H}]$ with respect to it [25]. One advantage of taking a harmonic potential is that $F_{\mathcal{H}}$ and $\rho_{\mathcal{H}}(\mathbf{R})$ can be expressed in a closed form in terms of the phonon frequencies and polarizations [31]. In particular, $\rho_{\mathcal{H}}(\mathbf{R})$ is Gaussian and is given as

$$\rho_{\mathcal{H}}(\mathbf{R}) = A_{\mathcal{H}} \exp\left[- \sum_{st\alpha\beta\mu} \frac{\sqrt{M_s M_t}}{2a_{\mu\mathcal{H}}^2} \epsilon_{\mu\mathcal{H}}^{s\alpha}\epsilon_{\mu\mathcal{H}}^{t\beta} u^{s\alpha} u^{t\beta} \right], \tag{2}$$

where $A_{\mathcal{H}}$ is the normalization constant, s and t are atom indices, α and β are Cartesian indices, μ is a mode index, M denotes the mass of an atom, $\mathbf{u} = \mathbf{R} - \mathbf{R}_{eq}$ is the displacement from equilibrium, $a_{\mu\mathcal{H}}^2 = \hbar \coth(\beta\hbar\omega_{\mu\mathcal{H}}/2)/(2\omega_{\mu\mathcal{H}})$, and $\{\omega_{\mu\mathcal{H}}\}$ and $\{\epsilon_{\mu\mathcal{H}}^{s\alpha}\}$ represent the phonon frequencies and polarizations defined by $\mathcal{H}$.

As long as the equilibrium positions are fixed by symmetry, as in PHs, minimizing $\mathcal{F}_H[\mathcal{H}]$ with respect to $\mathcal{V}$ is equivalent to performing the minimization with respect to the force constant matrix C, which defines the trial harmonic potential as $\mathcal{V} = \frac{1}{2}\sum_{st\alpha\beta} u^{s\alpha} C_{st}^{\alpha\beta} u^{t\beta}$. The minimization is carried through the components of C in the basis of $N \times N$ Hermitian matrices preserving crystal symmetries, where N is the number of modes. We minimize $\mathcal{F}_H[\mathcal{H}]$ by a conjugate-gradient (CG) algorithm, which requires the knowledge of the gradient $\boldsymbol{\nabla}\mathcal{F}_H[\mathcal{H}]$ with respect to C:

$$\boldsymbol{\nabla}\mathcal{F}_H[\mathcal{H}] = -\sum_{st\alpha\beta} E_{\mathcal{H}}^{st\alpha\beta} \int d\mathbf{R}\, \tilde{f}_{\mathcal{H}}^{s\alpha}(\mathbf{R}) u^{t\beta} \rho_{\mathcal{H}}(\mathbf{R}), \tag{3}$$

where $E_{\mathcal{H}}^{st\alpha\beta} = \sum_{\mu}\sqrt{M_t/M_s}(\epsilon_{\mu\mathcal{H}}^{s\alpha}\boldsymbol{\nabla}\ln a_{\mu\mathcal{H}} + \boldsymbol{\nabla}\epsilon_{\mu\mathcal{H}}^{s\alpha})\epsilon_{\mu\mathcal{H}}^{t\beta}$, and $\tilde{f}_{\mathcal{H}}^{s\alpha}(\mathbf{R}) = f^{s\alpha}(\mathbf{R}) - f_{\mathcal{H}}^{s\alpha}(\mathbf{R})$ is the difference between the force on the sth atom along the direction α, $f^{s\alpha}(\mathbf{R})$, and the harmonic force derived from $\mathcal{V}$, $f_{\mathcal{H}}^{s\alpha}(\mathbf{R})$. At each step j of the CG minimization, the trial harmonic Hamiltonian is updated to $\mathcal{H}_j$, until the minimum is found. At the minimum, the $\{\omega_{\mu\mathcal{H}}\}$ frequencies form the SCHA phonon spectrum renormalized by anharmonicity

In our stochastic SCHA (SSCHA) approach, both $\mathcal{F}_H[\mathcal{H}]$ and $\boldsymbol{\nabla}\mathcal{F}_H[\mathcal{H}]$ are calculated making use of importance sampling and reweighting techniques. We start defining an initial trial $\mathcal{H}_0$ harmonic Hamiltonian and creating a set of $\{\mathbf{R}_I\}_{I=1,...,N_c}$ ionic configurations in a supercell according to the $\rho_{\mathcal{H}_0}(\mathbf{R})$ distribution given in Eq. (2). These configurations are trivially created making use of random numbers generated with a Gaussian distribution. Secondly, we calculate the BO energy and the atomic forces for each random configuration $\mathbf{R}_I$, $V(\mathbf{R}_I)$, and $f^{s\alpha}(\mathbf{R}_I)$, respectively. This allows us to evaluate the integrals in Eqs. (1) and (3) as an average of the integrands over the N_c configurations (importance sampling). Thus, we can compute the free energy and its gradient, and perform the first CG step to obtain $\mathcal{H}_1$. In principle we should reevaluate BO energies and forces for the supercell at each CG step j, a very time-demanding task as generally hundreds of steps are needed to converge. This can be avoided with a reweighting procedure. We introduce the reweighting $\rho_{\mathcal{H}_j}(\mathbf{R}_I)/\rho_{\mathcal{H}_0}(\mathbf{R}_I)$ factor (equal to one in the first $j = 0$ step) in the importance sampling evaluation of the integrals. Namely, $\mathcal{F}_H[\mathcal{H}_j]$ and $\boldsymbol{\nabla}\mathcal{F}_H[\mathcal{H}_j]$ are obtained as

$$\mathcal{F}_H[\mathcal{H}_j] \simeq F_{\mathcal{H}_j} + \frac{1}{N_c}\sum_{I=1}^{N_c}[V(\mathbf{R}_I) - \mathcal{V}_j(\mathbf{R}_I)]\frac{\rho_{\mathcal{H}_j}(\mathbf{R}_I)}{\rho_{\mathcal{H}_0}(\mathbf{R}_I)}, \tag{4}$$

$$\boldsymbol{\nabla}\mathcal{F}_H[\mathcal{H}_j] \simeq -\sum_{st\alpha\beta} E_{\mathcal{H}_j}^{st\alpha\beta}\frac{1}{N_c}\sum_{I=1}^{N_c}\tilde{f}_{\mathcal{H}_j}^{s\alpha}(\mathbf{R}_I)u_I^{t\beta}\frac{\rho_{\mathcal{H}_j}(\mathbf{R}_I)}{\rho_{\mathcal{H}_0}(\mathbf{R}_I)}, \tag{5}$$

where the equality holds for $N_c \to \infty$. Including the reweighting factor, we can use the BO energies and forces of the configurations created with the initial $\rho_{\mathcal{H}_0}(\mathbf{R})$ distribution also for the following j CG iterations. However, if $(1/N_c)\sum_{i=1}^{N_c}\rho_{\mathcal{H}_j}(\mathbf{R}_i)/\rho_{\mathcal{H}_0}(\mathbf{R}_i)$ deviates substantially from one, $\mathcal{F}_H[\mathcal{H}_j]$ and $\boldsymbol{\nabla}\mathcal{F}_H[\mathcal{H}_j]$ cannot be accurately evaluated anymore as the initial set of configurations does not represent closely $\rho_{\mathcal{H}_j}(\mathbf{R})$. When this occurs, we use the probability distribution of the current step $\rho_{\mathcal{H}_j}(\mathbf{R})$ to create a new set of configurations for which we recompute atomic forces and BO energies to be used in the present and subsequent CG iterations. The process continues until the gradient vanishes.

We apply this method to stoichiometric PdH, PdD, and PdT. Total energies, atomic forces, harmonic phonons, and deformation potentials needed for the Eliashberg functions are computed with density-functional theory and linear response [32,33]. We use the Perdew-Zunger local-density approximation [34] and ultrasoft pseudopotentials [35].

We first demonstrate the capability of our developed method to obtain the free energy as a function of temperature. We calculate $\mathcal{F}_H[\mathcal{H}]$ and $\boldsymbol{\nabla}\mathcal{F}_H[\mathcal{H}]$ from a model potential combining the *ab initio* harmonic potential with a fourth-order on-site anharmonic potential fitted to the density-functional theory total energies [36]. The potential

satisfies the symmetries of the rock-salt structure [18] and
has also been used to study cubic ferroelectrics [37]. In this
system anharmonic forces are short range and, conse-
quently, phonon dispersions calculated with the model
potential and with *ab initio* forces are in close agreement
(see the Supplemental Material [38]). The use of the model
allows us to estimate the free energy at several volumes and
temperatures very efficiently. Minimizing the free energy
we obtain the lattice parameter of each isotope as a function
of temperature. The absolute values of the lattice parameters
and the thermal expansion coefficients (see Fig. 1) are in
good agreement with measurements [12,20,39].

Once the equilibrium volumes are determined, we
obtain the SSCHA phonon dispersions computing the
forces on the $\{\mathbf{R}_I\}_{I=1,...,N_c}$ configurations completely from
first principles [36], overcoming the approximation of a
model potential. The results are shown in Fig. 2 and
compared with available experimental data on deuterium
and tritium deficient samples. The breakdown of the har-
monic approximation is evident in all systems, particularly
in PdH and PdD displaying imaginary phonon frequencies.
The anharmonic correction given by the SSCHA is larger
than the harmonic phonon frequency itself, invalidating
any possible perturbative approach. Interestingly, both
the low-energy acoustic and high-energy optical modes
are affected by anharmonicity even if the largest correction
involves the H-character optical modes. At zone center the
PdH optical modes are degenerate at 488 cm^{-1}, in good
agreement with inelastic neutron and Raman experiments
[10–13] (around 450–472 cm^{-1} at different temperatures
and H concentrations). Since the H atom is smaller than the
octahedral void in the Pd fcc lattice, hydrogen vibrations
are characterized by very anharmonic rattling modes. This
is confirmed by the weak mass dependence of the root-
mean square displacement of hydrogen (0.55 a.u. in PdH,

0.48 a.u. in PdD, and 0.44 a.u. in PdT at 0 K), which does
not scale according to the harmonic $M^{-0.5}$ relation.

From the calculated phonon spectra we obtain the
Eliashberg function as

$$\alpha^2 F(\omega) = \frac{1}{N(0)N_k N_q} \sum_{\mathbf{kq}nm} \sum_{st\alpha\beta\mu} \frac{\epsilon_\mu^{s\alpha}(\mathbf{q})\epsilon_\mu^{t\beta*}(\mathbf{q})}{2\omega_\mu(\mathbf{q})\sqrt{M_s M_t}}$$
$$\times d_{\mathbf{k}n,\mathbf{k}+\mathbf{q}m}^{s\alpha} d_{\mathbf{k}n,\mathbf{k}+\mathbf{q}m}^{t\beta*} \delta(\epsilon_{\mathbf{k}n})\delta(\epsilon_{\mathbf{k}+\mathbf{q}m})$$
$$\times \delta(\omega - \omega_\mu(\mathbf{q})), \qquad (6)$$

FIG. 2 (color online).   Harmonic and SSCHA phonon spectra
calculated for PdH (a), PdD (b), and PdT (c) at the equilibrium
volume at 0 K. The experimental results obtained for nonstoi-
chiometric PdD$_{0.63}$ [14] and PdT$_{0.70}$ [15] are shown. In the right
panels the PDOS projected onto Pd and H atoms is plotted within
the harmonic approximation (dotted lines) and the SSCHA
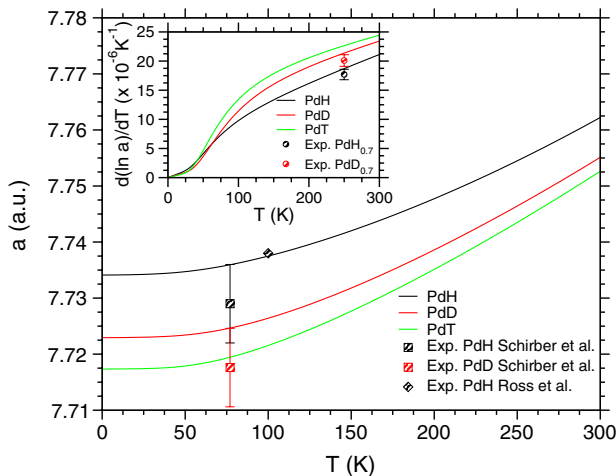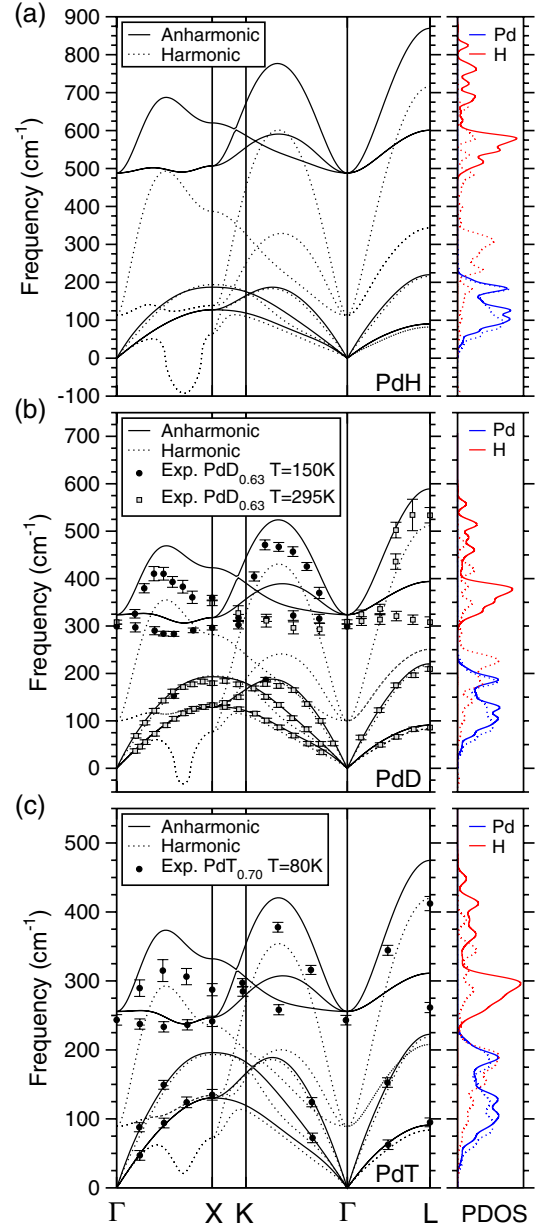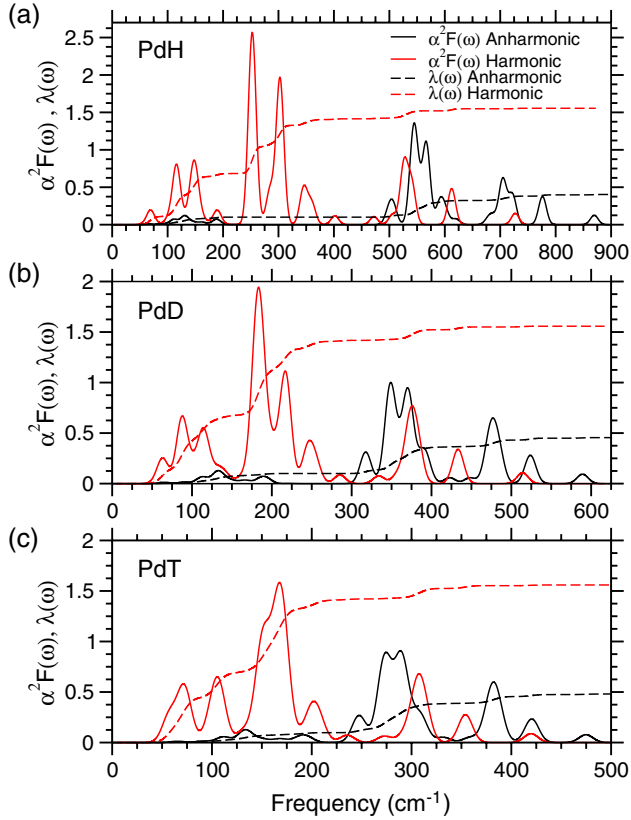(solid lines).

FIG. 1 (color online).   Equilibrium lattice parameters as a
function of temperature for PdH, PdD, and PdT compared to
experimental results [12,20]. In the inset the calculated thermal
expansion coefficients are shown together with the measured
values in Ref. [39].

FIG. 3 (color online). $\alpha^2 F(\omega)$ and $\lambda(\omega) = 2\int_0^\omega d\omega'\alpha^2 F(\omega')/\omega'$ for (a) PdH, (b) PdD, and (c) PdT within the harmonic approximation and the SSCHA.

where $d^{s\alpha}_{\mathbf{k}n,\mathbf{k}+\mathbf{q}m} = \langle\mathbf{k}n|\delta V/\delta u^{s\alpha}(\mathbf{q})|\mathbf{k}+\mathbf{q}m\rangle$ is the deformation potential, $|\mathbf{k}n\rangle$ is a Kohn-Sham state with energy $\epsilon_{\mathbf{k}n}$ measured from the Fermi level ϵ_F, N_k and N_q are the number of electron and phonon momentum points used for the Brillouin-zone (BZ) sampling, and $N(0)$ is the density of states per spin at ϵ_F. We compute $\alpha^2 F(\omega)$ in the harmonic or anharmonic case by using the harmonic or SSCHA phonon frequencies and polarizations in Eq. (6). The electron-phonon coupling constant λ, as well as the logarithmic frequency average $\omega_{\log}$, are obtained as $\lambda = 2\int_0^\infty d\omega \alpha^2 F(\omega)/\omega$ and $\omega_{\log} = \exp(2/\lambda \int_0^\infty d\omega \alpha^2 F(\omega) \times \ln\omega/\omega)$ [40]. We estimate T_c from the solution of the single-band Migdal-Eliashberg equations, using $\mu^* = 0.085$ as calculated in Ref. [17]. In the harmonic approximation the equilibrium volume of PdT is used for all isotopes as, in this case, there are no imaginary phonons. $\alpha^2 F(\omega)$ functions are shown in Fig. 3 and the results for T_c are presented in Table I.

In the harmonic approximation λ is independent of the mass and the isotope coefficient is determined by $\omega_{\log}$. Thus, the heavier the isotope the lower T_c and α is close to 0.5. The harmonic approximation strongly overestimates T_c, predicting very high values for all compounds. This overestimation is due to the very soft H-character vibrations that contribute as $\lambda \propto \omega^{-2}$ to the electron-phonon coupling, leading to extraordinary values for λ. This is

TABLE I. Calculated λ, $\omega_{\log}$, and T_c values for PHs. $\omega_{\log}$ values are given in cm^{-1} and T_c's in K. Experimental values for T_c [6,7] are presented as well. The value of α between isotopes PdA and PdB is calculated as $\alpha_{\text{PdA(B)}} = -(\ln T_c(\text{PdB}) - \ln T_c(\text{PdA}))/(\ln M_B - \ln M_A)$.

	Harmonic			SSCHA			Expt.	
	λ	$\omega_{\log}$	T_c	λ	$\omega_{\log}$	T_c	T_c [6]	T_c [7]
PdH	1.55	205	47	0.40	405	5.0	9	8
PdD	1.55	150	34	0.46	304	6.5	11	10
PdT	1.55	125	30	0.48	257	6.9		
$\alpha_{\text{PdH(D)}}$		0.47				-0.38	-0.29	-0.32
$\alpha_{\text{PdH(T)}}$		0.41				-0.29		

evident from the comparison between the phonon density of states (PDOS) (see Fig. 2) and $\alpha^2 F(\omega)$ (see Fig. 3).

In the SSCHA, both λ, and consequently T_c, are substantially reduced due to the enhancement of the frequencies induced by anharmonicity. The hardening is more important the lighter the isotope as lighter atoms feel the potential farther away from equilibrium because of the fluctuations of the zero-point motion. This makes λ mass dependent and larger the heavier the isotope. Remarkably, the differences in λ explain the inverse isotope effect in T_c and the value we obtain for the isotope coefficient α is in good agreement with experiments (see Table I). The obtained T_c's are close to experimental results even if no anharmonic corrections were incorporated into the deformation potential. As noted by $\alpha^2 F(\omega)$ and the integrated electron-phonon coupling $\lambda(\omega)$ in Fig. 3, H-character optical modes have the largest contribution to λ, between 75% and 79% of the total depending on the isotope. The contribution of the low-energy Pd-character acoustic modes is similar for the three hydrides. Thus, we conclude that superconductivity and the inverse isotope effect in PHs is driven by hydrogen anharmonicity.

In summary, we present a stochastic implementation of the SCHA that allows us to treat anharmonic effects in the nonperturbative regime. The method gives access directly to the free energy of the system and is variational in the free energy with respect to a trial harmonic Hamiltonian. The method is applied to PHs calculating the free energy, the thermal expansion, the anharmonic phonon spectra, and the superconducting properties. We demonstrate that superconductivity in PHs is phonon mediated and the anomalous inverse isotope effect is due to the large anharmonicity of hydrogen vibrations, which is impossible to treat within perturbation theory. Our findings open new perspectives in the interpretation of reduced isotope effects in superconductors. Moreover, we demonstrate that anharmonicity induces a huge suppression of T_c, almost a factor of 10 in PdH. This poses the question of whether harmonic T_c calculations in high-pressure metallic hydrides [41] are overestimated [22], in particular, in the very similar PtH [42]. More generally, our methodological developments will allow us to investigate strongly anharmonic systems

[1] J. Bardeen, L. N. Cooper, and J. R. Schrieffer, Phys. Rev. **108**, 1175 (1957).

[2] D. G. Hinks, H. Claus, and J. D. Jorgensen, Nature (London) **411**, 457 (2001).

[3] M. S. Fuhrer, K. Cherrey, A. Zettl, M. L. Cohen, and V. H. Crespi, Phys. Rev. Lett. **83**, 404 (1999).

[4] B. Batlogg, R. J. Cava, A. Jayaraman, R. B. van Dover, G. A. Kourouklis, S. Sunshine, D. W. Murphy, L. W. Rupp, H. S. Chen, A. White, K. T. Short, A. M. Mujsce, and E. A. Rietman, Phys. Rev. Lett. **58**, 2333 (1987).

[5] R. H. Liu, T. Wu, G. Wu, H. Chen, X. F. Wang, Y. L. Xie, J. J. Ying, Y. J. Yan, Q. J. Li, B. C. Shi, W. S. Chu, Z. Y. Wu, and X. H. Chen, Nature (London) **459**, 64 (2009).

[6] B. Stritzker and W. Buckel, Z. Phys. **257**, 1 (1972).

[7] J. E. Schirber and C. J. M. Northrup, Phys. Rev. B **10**, 3818 (1974).

[8] J. E. Schirber, J. M. Mintz, and W. Wall, Solid State Commun. **52**, 837 (1984).

[9] A. E. Karakozov and E. G. Maksimov, Zh. Eksp. Teor. Fiz. **74**, 681 (1978).

[10] A. Kolesnikov, I. Natkaniec, V. Antonov, I. Belash, V. Fedotov, J. Krawczyk, J. Mayer, and E. Ponyatovsky, Physica (Amsterdam) **174B**, 257 (1991).

[11] R. Sherman, H. K. Birnbaum, J. A. Holy, and M. V. Klein, Phys. Lett. **62A**, 353 (1977).

[12] D. K. Ross, V. E. Antonov, E. L. Bokhenkov, A. I. Kolesnikov, E. G. Ponyatovsky, and J. Tomkinson, Phys. Rev. B **58**, 2591 (1998).

[13] M. Chowdhury and D. Ross, Solid State Commun. **13**, 229 (1973).

[14] J. M. Rowe, J. J. Rush, H. G. Smith, M. Mostoller, and H. E. Flotow, Phys. Rev. Lett. **33**, 1297 (1974).

[15] J. M. Rowe, J. J. Rush, J. E. Schirber, and J. M. Mintz, Phys. Rev. Lett. **57**, 2955 (1986).

[16] R. J. Miller and C. B. Satterthwaite, Phys. Rev. Lett. **34**, 144 (1975).

[17] B. M. Klein, E. N. Economou, and D. A. Papaconstantopoulos, Phys. Rev. Lett. **39**, 574 (1977).

[18] C. Elsässer, K. M. Ho, C. T. Chan, and M. Fähnle, Phys. Rev. B **44**, 10 377 (1991).

[19] B. M. Klein and R. E. Cohen, Phys. Rev. B **45**, 12 405 (1992).

[20] J. E. Schirber and B. Morosin, Phys. Rev. B **12**, 117 (1975).

[21] P. Jena, J. Jones, and R. M. Nieminen, Phys. Rev. B **29**, 4140 (1984).

[22] B. Rousseau and A. Bergara, Phys. Rev. B **82**, 104504 (2010).

[23] L. Paulatto, F. Mauri, and M. Lazzeri, Phys. Rev. B **87**, 214303 (2013).

[24] M. Lazzeri and S. de Gironcoli, Phys. Rev. B **65**, 245402 (2002).

[25] D. J. Hooton, Philosophical Magazine Series 7 **46**, 422 (1955).

[26] P. Souvatzis, O. Eriksson, M. I. Katsnelson, and S. P. Rudin, Phys. Rev. Lett. **100**, 095901 (2008).

[27] O. Hellman, I. A. Abrikosov, and S. I. Simak, Phys. Rev. B **84**, 180301 (2011).

[28] B. Monserrat, N. D. Drummond, and R. J. Needs, Phys. Rev. B **87**, 144302 (2013).

[29] I. Errea, B. Rousseau, and A. Bergara, Phys. Rev. Lett. **106**, 165501 (2011).

[30] I. Errea, B. Rousseau, and A. Bergara, J. Appl. Phys. **111**, 112604 (2012).

[31] S. Rossano, F. Mauri, C. J. Pickard, and I. Farnan, J. Phys. Chem. B **109**, 7245 (2005).

[32] P. Giannozzi et al., J. Phys. Condens. Matter **21**, 395502 (2009).

[33] S. Baroni, S. de Gironcoli, A. D. Corso, and P. Giannozzi, Rev. Mod. Phys. **73**, 515 (2001).

[34] J. P. Perdew and A. Zunger, Phys. Rev. B **23**, 5048 (1981).

[35] Calculations are performed applying the QUANTUM-ESPRESSO [32] code. A 50 Ry cutoff is used for the plane-wave basis and a $24 \times 24 \times 24$ mesh for the BZ integrations in the unit cell. The sum over **k** in Eq. (6) required a $72 \times 72 \times 72$ grid.

[36] Total energies and forces needed in Eqs. (4) and (5) are computed in a $2 \times 2 \times 2$ supercell containing 16 atoms. The difference between the SSCHA force constant matrix and the harmonic force constant matrix in the $2 \times 2 \times 2$ supercell is interpolated to a $4 \times 4 \times 4$ supercell. The harmonic $4 \times 4 \times 4$ force constant matrix is added to the result. We verified that the anharmonic phonon dispersion obtained for the model potential in this way coincides with that obtained directly in a $4 \times 4 \times 4$ supercell. We use $N_c = 20000$ and $N_c = 300$ for the calculations with the model and *ab initio* potential, respectively. For the *ab initio* calculation a single set $\{\mathbf{R}_I\}_{I=1,...,N_c}$ is sufficient if the result of the model potential is used as $\mathcal{H}_0$.

[37] W. Zhong, D. Vanderbilt, and K. M. Rabe, Phys. Rev. B **52**, 6301 (1995).

[38] See Supplemental Material at http://link.aps.org/supplemental/10.1103/PhysRevLett.111.177002 for a description of the model potential.

[39] R. Abbenseth and H. Wipf, J. Phys. F **10**, 353 (1980).

[40] P. B. Allen and R. C. Dynes, Phys. Rev. B **12**, 905 (1975).

[41] D. Y. Kim, R. H. Scheicher, H.-k. Mao, T. W. Kang, and R. Ahuja, Proc. Natl. Acad. Sci. U.S.A. **107**, 2793 (2010).

[42] D. Y. Kim, R. H. Scheicher, C. J. Pickard, R. J. Needs, and R. Ahuja, Phys. Rev. Lett. **107**, 117002 (2011).

[43] G. Grüner, *Density Waves in Solids* (Addison-Wesley, Reading, MA, 1994).